

## DNA-functionalized hydrogels for confined membrane-free *in vitro* transcription/translation†

Cite this: *Lab Chip*, 2014, 14, 2651

J. Thiele,<sup>\*a</sup> Y. Ma,<sup>a</sup> D. Foschepoth,<sup>a</sup> M. M. K. Hansen,<sup>a</sup> C. Steffen,<sup>b</sup> H. A. Heus<sup>a</sup> and W. T. S. Huck<sup>a</sup>

Received 21st December 2013,  
Accepted 17th February 2014

DOI: 10.1039/c3lc51427g

www.rsc.org/loc

We microfluidically fabricate bio-orthogonal DNA-functionalized porous hydrogels from hyaluronic acid that are employed in *in vitro* transcription/translation (IVTT) of a green fluorescent protein. By co-encapsulating individual hydrogel particles and the IVTT machinery in water-in-oil microdroplets, we study protein expression in a defined reaction volume. Our approach enables precise control over protein expression rates by gene dosage. We show that gene transcription and translation are confined to the membrane-free hydrogel matrix, which contributes to the design of membrane-free protocells.

### Introduction

Gene expression is the process in which genetic information is transferred into a gene product, usually proteins, through transcription of a gene into messenger RNA (mRNA) followed by mRNA translation by ribosomes into the encoded polypeptide.<sup>1,2</sup> In contrast to gene expression in the complex environment *in vivo*, *in vitro* transcription/translation (IVTT) that is mostly based on *Escherichia coli* (*E. coli*) cell lysates enables a high degree of control over individual reaction components including DNA templates, amino acids, cell lysate extract, buffer, energy regeneration systems and nucleoside triphosphates.<sup>3,4</sup> Conventional studies on *in vitro* gene expression are usually performed in dilute, homogeneous bulk solutions, which do not reflect the microscopic confinement *in vivo*.<sup>5,6</sup> Therefore reaction and diffusion times as well as production rates can differ strongly between cell-free and in-cell biological processes.<sup>7–9</sup> On this account, it was recently demonstrated that coacervates of poly(ethylene glycol) (PEG) and cell lysates as well as polyelectrolytes and nucleotides can serve as crowded microcompartments for IVTT and enzymatic reactions, respectively.<sup>10,11</sup> While the process of coacervation has great potential in designing membrane-free compartments for biological processes, it relies on an undirected assembly thus offering limited control over the microstructure of the microcompartments or the spatial organization of key components

therein. As alternatives, biocompatible, polymeric hydrogel particles produced by droplet-based microfluidics utilizing bio-orthogonal chemistry have great advantages in the directed generation of microcompartments with controlled size, defined microarchitecture and desired functionality.<sup>12–16</sup>

Here, we present the preparation of DNA-functionalized hyaluronic acid hydrogel microparticles by droplet microfluidics to spatially confine gene expression in a tailor-made hydrogel matrix with sizes in the range of living cells. To ensure the free diffusion of key components of the IVTT machinery throughout the hydrogel matrix, bio-orthogonal thiol-ene chemistry is employed to form hydrogels from poly(ethylene glycol) diacrylate (PEGDA) cross-linked thiol-modified hyaluronic acid, which have been previously reported to possess large pore sizes of up to several hundred nanometers.<sup>17,18</sup> A DNA template encoding for a green fluorescent protein is covalently attached to the porous hydrogel matrix to confine the transcription/translation process to the hydrogel matrix. Subsequently, IVTT inside individual DNA-functionalized hydrogel particles (HA-S-DNA) is studied by microfluidically co-encapsulating hydrogel particles and an IVTT machinery in water-in-oil microdroplets. This allows us to follow gene expression in membrane-free compartments made from hydrogel microparticles in the defined volume of microdroplets.

### Results and discussion

We perform gene expression based on a commercial IVTT kit using a truncated gene of an enhanced green fluorescent protein (deGFP) sub-cloned into a pRSET5d vector.<sup>19</sup> By using a phosphoramidite-functionalized oligonucleotide, the DNA template is chemically coupled to the hydrogel, as sketched in Fig. 1A, upper panel. A second Alexa 647-tagged primer on

<sup>a</sup> Radboud University Nijmegen, Institute for Molecules and Materials, Heyendaalseweg 135, 6525 AJ Nijmegen, The Netherlands.  
E-mail: j.thiele@science.ru.nl

<sup>b</sup> Rhine-Waal University of Applied Sciences, Marie-Curie-Strasse 1, 47533 Kleve, Germany

† Electronic supplementary information (ESI) available: Experimental details on DNA fragment design (cloning experiments and PCR). See DOI: 10.1039/c3lc51427g

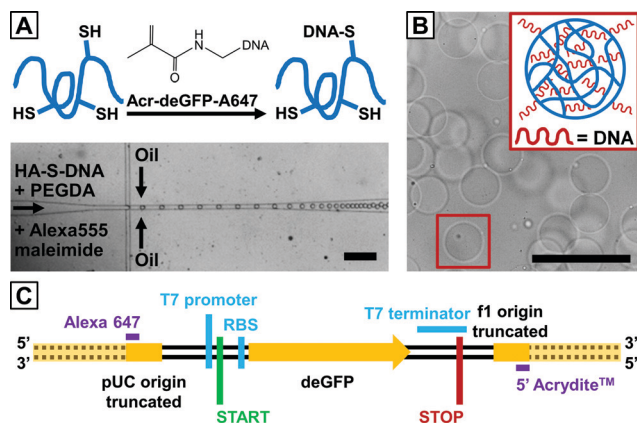


**Fig. 1** Fabrication of fluorescently labelled, DNA functionalized hyaluronic acid hydrogel microparticles. (A) Functionalization of thiol-modified hyaluronic acid with phosphoramidite DNA to give HA-S-DNA and its subsequent cross-linking with poly(ethylene glycol) diacrylate (PEGDA) and labelling using thiol-reactive Alexa 555 maleimide in a microfluidic flow focusing device. The scale bar denotes 150  $\mu\text{m}$ . (B) Bright-field microscope image of obtained monodisperse DNA-functionalized hyaluronic acid hydrogel particles swollen in water. The scale bar is 50  $\mu\text{m}$ . (C) A schematic drawing of DNA used in this study: linear DNA fragment of 1441 base pairs with a phosphoramidite (Acrydite™) linker at the 5' end of the template strand and an Alexa 647 tag on the 5' end of the coding strand.

the complementary strand of the DNA template allows us to fluorescently detect the presence of DNA in the hydrogel, as shown in Fig. 1C. Since the DNA fragment solely encodes deGFP, it is significantly smaller (1441 base pairs, bps) than the original plasmid DNA of approximately 3500 bps, which helps to improve the coupling efficiency to the hydrogel matrix.

To make DNA available for transcription throughout the hydrogel matrix, we require a polymer network porous enough to allow for the free diffusion of all components of the IVTT machinery. Initial attempts focusing on poly(acrylamide) hydrogels that can be easily customized by droplet microfluidics only gave hydrogels with pore sizes of a few nanometers and low DNA coupling efficiency, which is attributed to the dense polymer network resulting from the end-cross-linked low-molecular-weight monomer (J. Thiele, unpublished data). We thus employ a thiol-modified hyaluronic acid (HA-SH) macromonomer as the hydrogel precursor.<sup>20</sup> HA-SH is reacted with the DNA template that is modified with a phosphoramidite (Acrydite™) group, as shown in Fig. 1C, *via* Michael addition. Pre-incubation of both components improves their coupling efficiency and avoids competitive reactions with PEGDA, which is used in a subsequent step as a cross-linker sharing the same coupling chemistry.<sup>21,22</sup> The resulting PEGDA-cross-linked hyaluronic acid polymer network is more stable against degradation than a hydrogel solely cross-linked by disulfide bridges that are subjected to enzymatic degradation.<sup>23–25</sup> By employing droplet microfluidics, DNA-functionalized hydrogel microparticles with an average size of 20  $\mu\text{m}$  are formed, as shown in Fig. 1B. While aqueous suspensions of hyaluronic acid

hydrogel particles are visible under white light,<sup>26</sup> they are refractive index-matched in solutions of the IVTT machinery. We thus add thiol-reactive Alexa 555 maleimide to HA-S-DNA and PEGDA to fluorescently functionalize the HA-S-DNA/PEGDA hydrogel, which can later be independently detected from deGFP and the DNA template.

To determine the pore size of HA-S-DNA particles, we perform diffusion studies with fluorescein-labeled dextran (with a  $M_w$  of  $\sim 2 \times 10^6$  g mol<sup>-1</sup>) and Alexa 647-labeled prokaryotic 70S ribosomes with hydrodynamic diameters of approximately 54 nm and 30 nm, respectively.<sup>27,28</sup> Excess fluorescent tracers are removed by washing the dextran-bead solution with water, while the ribosome-bead solution is treated with magnesium-containing buffer to avoid disassembly of the ribosomes into their significantly smaller 30S and 50S subunits.<sup>29</sup> Confocal fluorescence microscopy images are taken immediately afterwards (Fig. 2, left). We indeed observe an increase in fluorescence intensity inside the hydrogel particles relative to the background, as shown by the line scans through hydrogel particles in Fig. 2, right. This indicates that the DNA-functionalized hyaluronic acid-based hydrogels are porous enough to allow for the free diffusion even of large assemblies in the IVTT mixture.

To monitor gene expression in individual hydrogel micro-compartments, a defined amount of hydrogel particles is added to a commercial IVTT mixture and compartmentalized into droplets with an average size of 60  $\mu\text{m}$  (Fig. 3). The output of the microfluidic particle-encapsulation device is directly fed into microfluidic chambers that enable fluorescence imaging over several hours under static conditions without significant droplet shrinkage due to water evaporation. For each experiment, a representative population of 50  $\mu\text{L}$  of hydrogel-bead containing microdroplets loaded with an IVTT mixture is collected. By encapsulating the hydrogel particles as well as collecting the hydrogel bead-containing emulsion at 4 °C, we ensure that the onset of *in vitro* transcription is delayed until the emulsion is imaged under the fluorescence microscope at room temperature (approximately 20 °C). As shown in Fig. 3B, left, the water-in-oil emulsion shows excellent monodispersity, as indicated by their hexagonal packing, and provides a defined volume of an IVTT mixture that can be taken up by the membrane-free hydrogel matrix thus improving the reproducibility of the experiments.

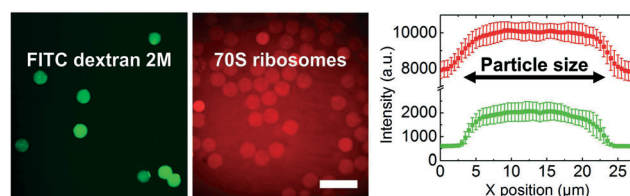


**Fig. 2** Characterization of the porosity of HA-S-DNA hydrogel particles by confocal fluorescence microscopy *via* diffusion of fluorescent probes of varying hydrodynamic diameters. Left: confocal fluorescence images; right: corresponding fluorescence intensity of line scans ( $N_{\text{BEAD}} = 50$ ). The scale bar for both panels denotes 50  $\mu\text{m}$ .

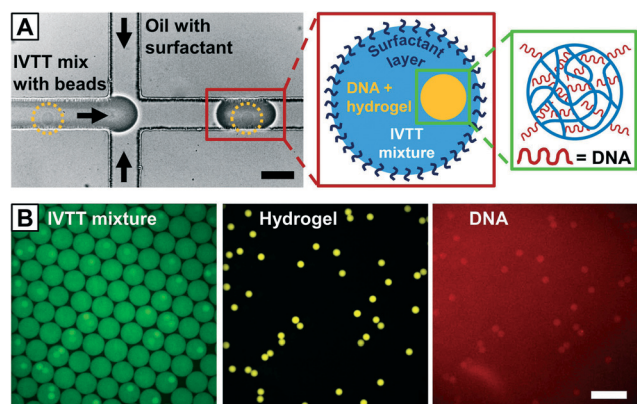


**Fig. 3** Fabrication and imaging of the HA-S-DNA hydrogel-loaded water-in-oil emulsion. (A) Encapsulation of HA-S-DNA hydrogel micro-particles into IVTT-containing microdroplets using a microfluidic flow focusing device. The scale bar is 50  $\mu\text{m}$ . (B) Fluorescence images of hydrogel particles encapsulated in microdroplets. Multi-channel acquisition of deGFP (IVTT kit; green channel), Alexa 555 (hydrogel; yellow channel) and Alexa 647 (DNA; red channel). Hexagonal packing of droplets indicates monodispersity. The scale bar for all panels is 100  $\mu\text{m}$ .

The water-in-oil emulsion remains stable for at least 4 hours which allows us to follow the IVTT process until protein production terminates, as discussed below. Multi-channel confocal fluorescence images of an average number of 250 droplets are recorded in each experiment at different time points using the green channel for detecting deGFP fluorescence as an indicator of protein production during the IVTT reaction, the yellow channel (Alexa 555) for determining the number of hydrogel particles inside the microdroplets, and the red channel (Alexa 647) for determining the relative concentration of DNA inside the hydrogel particles. A representative series of confocal fluorescence microscopy images of deGFP expression in the hydrogel-loaded droplets is presented in Fig. 4A, with all droplets displaying green fluorescence. However, a careful examination on the images reveals an increase in green fluorescence intensity only from HA-S-DNA particles-containing droplets. The fluorescence signal from the droplets that do not contain HA-S-DNA hydrogel particles is believed to originate from the auto-fluorescence of the IVTT mixture, whose intensity does not increase over time. It should be noted that initially ( $t = 0$  min.), HA-S-DNA particles appear to be slightly brighter than the surrounding IVTT mixture due to the likely non-specific adsorption of IVTT components to the hydrogel matrix. Over the course of the experiments however, this compartmentalization in fluorescence vanishes due to freely diffusing deGFP that superimposes the auto-fluorescence of the IVTT machinery.

As shown in Fig. 4B, left, there is a clear correlation between deGFP expression and the number of beads encapsulated per microdroplet. We find that protein fluorescence across single droplets increases linearly with an increasing number of encapsulated HA-S-DNA particles and thus an increasing amount of DNA. For example, the fluorescence intensity of deGFP increases from approximately 1000 over

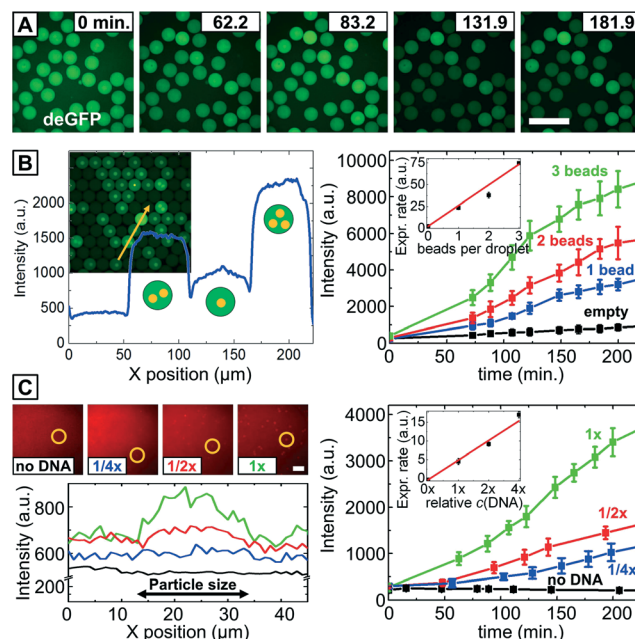


**Fig. 4** Expression of deGFP from HA-S-DNA hydrogel particles inside IVTT-kit-loaded microdroplets. (A) Confocal microscopy image sequence of deGFP fluorescence. (B) Fluorescence image overlay of deGFP and Alexa 555-labeled hydrogel particles and the corresponding line scan through droplets containing one, two, three or no HA-S-DNA particles, left panels; deGFP expression and expression rates depending on the number of HA-S-DNA particles per microdroplet, right. The scale bar for all panels in (A) is 200  $\mu\text{m}$ . (C) Fluorescence images of hydrogel particles with different concentrations of Alexa 647-labeled DNA, upper row; corresponding fluorescence intensity of line scans, lower row; deGFP expression and expression rates in single particle-loaded microdroplets depending on the DNA concentration per hydrogel particle, right. The scale bar for all panels denotes 100  $\mu\text{m}$ .

1500 to 2000 counts in droplets loaded with one, two and three HA-S-DNA hydrogel particles, respectively. The curves depicting temporal evolution of the average fluorescence intensity across the droplets exhibit a typical shape that is also obtained from bulk experiments.<sup>19</sup> The behaviour of the curves, shown in Fig. 4B, right, is characterized by a slow increase in fluorescence during mRNA production and an exponential increase due to protein production before it levels off as IVTT resources are exhausted. Protein expression kinetics are extracted by integrating the fluorescence intensity over the whole droplet volume from fluorescence images collected over time. As shown in the inset of Fig. 4B, right, not only the fluorescence intensity but also the rate of deGFP expression correlates linearly with the number of DNA-functionalized hydrogel particles encapsulated. As these results are consistent with previous studies on cell-free systems performed where DNA is homogeneously distributed throughout the reaction volume,<sup>30,31</sup> we can assume that the hydrogel-coupled DNA template is available for IVTT without restrictions.

The linear dependence of protein expression rates on the amount of DNA present in the hydrogel matrix is further studied by decreasing the relative amount of DNA in the

initial fabrication of the hydrogel particles which has been discussed in Fig. 1. By employing an Alexa 647-labeled DNA-template, we observe a decrease in fluorescence emission of the hydrogel matrix at 676/29 nm that expectedly correlates with the initial relative amount of DNA in the hydrogel production, as presented in Fig. 4C, left. Analyses of the images of IVTT experiments in microdroplets solely containing one bead show that a decrease in the amount of DNA to 1/2 and 1/4 of the original amount of DNA that has also been used in the experiments presented in Fig. 4B gives a similar linear relation of the protein expression rate and the DNA concentration as observed by varying the number of HA-S-DNA hydrogel particles. It is worth noting that deGFP production rates again stay in the linear regime within the DNA concentration range of our study, suggesting the transcription/translation machinery has never been saturated.<sup>19</sup>

To study the confinement of gene expression to our DNA-functionalized hydrogel in detail, we add a molecular beacon that contains a short methoxy-RNA nucleotide sequence with fluorescent Alexa 647 and dark quencher on either end that can hybridize to a specific part of a GFP-His mRNA sequence, and we repeat the experiment presented in Fig. 4A.<sup>10</sup> Upon binding to mRNA, the beacon changes its conformation from hairpin to linear, which displaces the quencher, rendering Alexa 647 fluorescent. As shown in Fig. 5A, left, DNA-S-HA particle-loaded droplets light up due to an increase in protein fluorescence over time, indicating that the transcription/translation machinery is active. However, there is no increase in Alexa 647 fluorescence in the same droplets, as shown by

line scans through single droplets (Fig. 5A, right). Since gene translation is obviously functional as we observe an increase in protein fluorescence signal, and an mRNA template is mandatory for the process of gene translation in the ribosomes, the stable fluorescent signal on the red channel indicates that the Alexa 647-labeled molecular beacon does not hybridize with its complementary mRNA sequence despite the obvious presence of mRNA. A closer look at single IVTT machinery-loaded hydrogels, Fig. 5B, reveals that the HA-S-DNA hydrogels also display significantly lower auto-fluorescence of the molecular beacon than the surrounding droplet volume, which is confirmed by the line scan, Fig. 5B, right. This suggests that mRNA encoding for GFP does not diffuse out of the hydrogel once transcription has occurred, nor during or after translation, since no increase in Alexa 647 fluorescence is observed over time outside the hydrogel particle due to the binding of a molecular beacon to mRNA. Therefore we are confident that both transcription and translation are confined to the hydrogel particle, thereby localizing the gene expression in a membrane-free compartment.<sup>10</sup>

## Conclusions

Porous DNA-functionalized hyaluronic acid hydrogel particles in the size range of living cells are employed as membrane-free microcompartments for confined gene expression and allow correlating protein expression rates with DNA concentrations. Gene expression rates inside the hydrogel particles increase linearly with increasing DNA concentrations within the DNA concentration range we have studied. Despite the porous hydrogel structure, experiments employing an mRNA targeting molecular beacon suggest that gene transcription is well confined to the hydrogel matrix, whereas the product of gene expression, deGFP, freely diffuses out of the hydrogel. By hydrogel engineering through bio-orthogonal thiol-ene chemistry, we develop a general approach for other DNA templates and biological processes beyond gene expression and provide the means for directed formation of membrane-free compartments with precise control over size, charge, density and hydrophobicity. This will likely contribute to the development of artificial cell-like platforms in the near future.<sup>32,33</sup>

## Materials and methods

### General experimental details

All reagents and chemicals were used as received unless otherwise specified. A commercial *in vitro* transcription/translation kit was purchased from 5PRIME (RTS 100 *Escherichia coli* HY kit). MilliQ water was obtained from a Labconco Water Pro PS purification system with a resistivity of 18.1 MΩ. Primer for DNA template design via PCR and the molecular beacon were obtained from Integrated DNA Technologies (Belgium). Samples were prepared in sterile Mars Safety Class 2 flow boxes (Scanlaf), and glassware was autoclaved. NMR spectra were recorded on a Varian Inova 400 spectrometer with D<sub>2</sub>O

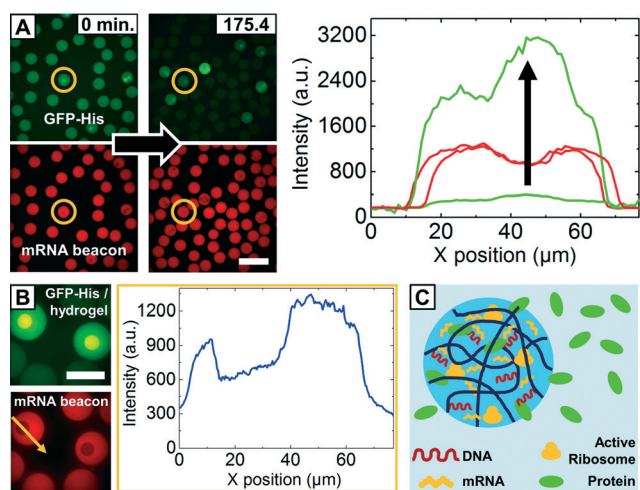


**Fig. 5** Utilization of a molecular beacon for the study of localized mRNA production in IVTT and HA-S-DNA hydrogel microparticles containing microdroplets. (A) Dual channel acquisition of GFP-His (green channel) and Alexa 647 mRNA beacon (red channel) signals during gene expression, left; line scans through highlighted droplets, right. The scale bar denotes 150 μm. (B) Fluorescence localization of GFP-His and hydrogel (upper left), Alexa 647-labeled molecular beacon (lower left) and corresponding line scan (right). The hydrogel particles are functionalized with a non-fluorescent DNA template to avoid fluorescence overlay with the molecular beacon. The scale bar is 50 μm. (C) A schematic demonstration of relative locations of key IVTT components inside a microdroplet containing a HA-S-DNA hydrogel particle.

as a solvent and TMS as an internal standard. Dialysis was performed in Spectra/Por® dialysis membranes ( $M_w$  cut-off: 3500 g mol<sup>-1</sup>). To determine the exact channel height of the channel network fabricated in SU-8 (Micro Resist Technology GmbH, Germany) *via* photolithography, differential interference contrast (DIC) microscopy was performed on a Wyco NT1100 optical profiler (Bruker, USA). Bright-field microscopy imaging was performed using an IX71 microscope (Olympus) equipped with 10× and 40× objective lenses (air) and a Phantom MIRO high-speed camera (Vision Research Inc., USA). Confocal microscopy measurements were performed using an Olympus IX81 confocal microscope, equipped with an Andor iXon3 camera, Andor 400-series solid-state lasers, and a Yokogawa CSU-X1 spinning disk unit. Fluorescein isothiocyanate (FITC) dextran and deGFP were excited at 488 nm and fluorescence emission detected using a 525/50 nm band pass filter. Alexa 555 and Alexa 647 were excited at 561 nm and 637 nm, respectively, and fluorescence emission was detected using 617/73 nm and 676/29 nm band pass filters, respectively.

### Microfluidic device fabrication and general microfluidic experimental setup

Microfluidic devices were fabricated using combined photo and soft lithography in poly(dimethylsiloxane) (PDMS) (Dow Corning, Germany).<sup>34</sup> A negative photoresist (SU-8 25 or SU-8 50, Microchem Co., USA) was spin-coated onto the polished site of a 2 inch silicon wafer (SI-MAT, Germany). A mask aligner (MJB3, Süss MikroTec, Germany) was used to impart the microchannel structure of a transparent photomask (JD Phototools, UK) into the photoresist. We optimized the master device fabrication employing DIC microscopy to obtain microchannels with a very uniform height of 23 μm for producing DNA-S-HA hydrogel particles and 50 μm for encapsulating hydrogel particles in IVTT mix-loaded microdroplets, respectively. The channel width at the droplet forming flow-focusing nozzle was 25 μm and 50 μm, respectively. A PDMS replica of the channel design was formed by mixing the PDMS oligomer and cross-linker in a ratio of 10:1 (w/w) and curing the homogeneous, degassed mixture at 65 °C for at least 60 min. Thereafter, access ports were bored into the soft replica with a biopsy needle (outer diameter: 1.0 mm, Pfm, Medical Workshop, USA), and the PDMS replica was bonded to a glass slide after oxygen plasma treatment. The bonding process was completed in an oven at 90 °C for approximately 1 h. Microfluidic devices were connected to high-precision, positive displacement syringe pumps (neMESYS, Cetoni, Germany) *via* PTFE tubing (inner diameter: 0.56 mm, outer diameter: 1.07 mm, Novodirect, Germany).

### Formation of DNA-functionalized hydrogel particles

Thiolated hyaluronic acid was synthesized following a modified procedure as previously reported by Prestwich and coworkers.<sup>35,36</sup> Briefly, 250 mg low molecular weight hyaluronic acid (sodium salt, Lifecore) with a  $M_w$  of ~50 kDa was dissolved in 25 mL MES buffer (pH 4.75), and 50 mg PDPH (Thermo Scientific) as

well as 300 mg 1-ethyl-3-(3-dimethylaminopropyl)carbodiimide (EDC) as solid was added sequentially. The reaction was carried out with stirring at room temperature for at least 2 h. The solution was dialyzed against MilliQ to remove excess reactants. Afterwards 100 mg tris(2-carboxyethyl)phosphine (TCEP) was added and the reaction mixture was stirred at room temperature for another 2 h. The solution was extensively dialyzed and, in a final step, lyophilized to give white solid thiolated hyaluronic acid. The degree of thiolation was measured by <sup>1</sup>H NMR and Ellman's test to be approximately 25%.<sup>37</sup>

To form DNA-functionalized hyaluronic acid-based hydrogel microparticles, a batch volume of typically 200 μL was made from 80 μL thiolated hyaluronic acid dissolved in autoclaved PBS buffer (4.5% w/w, pH 4.7) and 40 μL DNA template in water (*e.g.* 14.56 μg Acr-deGFP-A647, Fig. 4A), which was pre-incubated on a thermo shaker (Grant Bio PCMT, UK) at 37 °C for 75 min, before adding 80 μL of poly(ethylene glycol) diacrylate (575 g mol<sup>-1</sup>) dissolved in degassed PBS (0.3% w/w) and 0.5 μL Alexa Fluor® 555 C2 Maleimide (Life Technologies). The pink solution was injected into a microfluidic flow-focusing device with a height of 23 μm and a nozzle width of 25 μm as the inner phase together with fluorinated oil (HFE 7500, 3 M) containing 2% (w/w) of home-made triblock copolymer surfactant (Krytox-Jeffamine-Krytox) as the outer phase.<sup>38</sup> The flow rates were set to 660 μL h<sup>-1</sup> for the outer phase and 200 μL h<sup>-1</sup> for the inner phase. The emulsion was collected at 4 °C in an Eppendorf tube covered with Parafilm (Brand, Germany) and subsequently polymerized on a thermo shaker at 37 °C for 20 min and 60 °C for 40 min. Hydrogel particles were obtained by breaking the emulsion with 1*H*,1*H*,2*H*,2*H*-perfluoro-1-octanol (20% v/v in HFE 7500) and transferring the particles into water. The particle suspension was washed three times with aqueous L-glutamic acid potassium salt monohydrate (467 mmol) which had the same ionic strength as the commercial IVTT kit that was later employed,<sup>10</sup> and three times with plain water to remove any adhering and trapped DNA template that could later leak out of the hydrogel particles.

### Hydrogel particle encapsulation in IVTT solution

Hydrogel particles were encapsulated into IVTT-loaded microdroplets using the same setup for microfluidic experiments, as described above, but located in a cold room set to 4 °C. All consumables were equilibrated at 4 °C for 2 h. In detail, a homogeneous suspension of 120 μL of the IVTT mixture (three aliquots according to the 5Prime manual) was combined with 35 μL of DNA-functionalized hyaluronic acid-based hydrogel particles and stored on ice. The mixture was then injected into a microfluidic flow-focusing device with a height of 50 μm and a nozzle width of 50 μm as the inner phase together with fluorinated oil (HFE 7500, 3 M) containing 2% (w/w) of surfactant as the outer phase. The flow rates of the outer and inner phase were set to 600 μL h<sup>-1</sup> and 200 μL h<sup>-1</sup>, respectively, and the outlet stream of the microfluidic device was directly fed into a microfluidic

chamber device to avoid water evaporation and allow for long-term imaging, as shown in the ESI,† Fig. S3. The chambers were sealed with transparent tape and transferred to a confocal microscope where the samples warmed up to room temperature.

## Acknowledgements

We thank Ing. Frank H. T. Nelissen (Radboud University, IMM, Biophysical Chemistry) and Dr. Evan Spruijt (ESPCI ParisTech, France) for fruitful discussions, Emilien Dubuc (Radboud University, IMM, Physical-Organic Chemistry) for designing the molecular beacon, and Vincent Noireaux (University of Minnesota) for donating the gene of an enhanced green fluorescent protein. J. T. is a Feodor-Lynen fellow of the Alexander von Humboldt Foundation. Work in the Huck group was supported by a European Research Council (ERC) Advanced Grant (246812 Intercom), a VICI grant from the Netherlands Organization for Scientific Research (NWO), and by funding from the Ministry of Education, Culture and Science (Gravity program 024.001.035).

## Notes and references

- 1 T. A. Brown, *Genomes*, Garland Science, 3rd edn, 2006.
- 2 M. Kozak, *Gene*, 1999, **234**, 187; M. Kozak, *Gene*, 2005, **361**, 13.
- 3 A. S. Spirin, V. I. Baranov, L. A. Ryabova, S. Y. Ovodov and Y. B. Alakhov, *Science*, 1988, **242**, 1162.
- 4 L. Jermutus, L. A. Ryabova and A. Plückthun, *Curr. Opin. Biotechnol.*, 1998, **9**, 534.
- 5 P. M. Llopis, A. F. Jackson, O. Sliusarenko, I. Surovtsev, J. Heinritz, T. Emonet and C. Jacobs-Wagner, *Nature*, 2010, **466**, 77.
- 6 A. Köhler and E. Hurt, *Nat. Rev. Mol. Cell Biol.*, 2007, **8**, 761.
- 7 Y. Ben-Ari, Y. Brody, N. Kinor, A. Mor, T. Tsukamoto, D. L. Spector, R. H. Singer and Y. Shav-Tal, *J. Cell Sci.*, 2010, **123**, 1761.
- 8 S. Soh, M. Byrska, K. Kandere-Grzybowska and B. A. Grzybowski, *Angew. Chem., Int. Ed.*, 2010, **49**, 4170.
- 9 D. Cottrell, P. S. Swain and P. F. Tupper, *Proc. Natl. Acad. Sci. U. S. A.*, 2012, **109**, 9699.
- 10 E. Sokolova, E. Spruijt, M. M. K. Hansen, E. Dubuc, J. Groen, V. Chokkalingam, A. Piruska, H. A. Heus and W. T. S. Huck, *Proc. Natl. Acad. Sci. U. S. A.*, 2013, **110**, 11692.
- 11 J. Crosby, T. Treadwell, M. Hammerton, K. Vasilakis, M. P. Crump, D. S. Williams and S. Mann, *Chem. Commun.*, 2012, **48**, 11832–11834.
- 12 J. Heo and R. M. Crooks, *Anal. Chem.*, 2005, **77**, 6843.
- 13 C. Y. Li, D. K. Wood, C. M. Hsu and S. N. Bhatia, *Lab Chip*, 2011, **11**, 2967.
- 14 H. Zhang, G. Jenkins, Y. Zou, Z. Zhu and C. J. Yang, *Anal. Chem.*, 2012, **84**, 3599.
- 15 J. B. Lee, S. Peng, D. Yang, Y. H. Roh, H. Funabashi, N. Park, E. J. Rice, L. Chen, R. Long, M. Wu and D. Luo, *Nat. Nanotechnol.*, 2012, **7**, 816.
- 16 R. C. H. Ruiz, P. Kiatwuthinon, J. S. Kahn, Y. H. Roh and D. Luo, *Ind. Biotechnol.*, 2012, **8**, 372.
- 17 C. E. Hoyle and C. N. Bowman, *Angew. Chem., Int. Ed.*, 2010, **49**, 1540.
- 18 J. B. Leach, K. A. Bivens, C. W. Patrick, Jr. and C. E. Schmidt, *Biotechnol. Bioeng.*, 2003, **82**, 578.
- 19 J. Shin and V. Noireaux, *J. Biol. Eng.*, 2010, **4**, 1.
- 20 J. A. Burdick and G. D. Prestwich, *Adv. Mater.*, 2011, **23**, H41.
- 21 R. Jin, L. S. Moreira-Teixeira, A. Krouwels, P. J. Dijkstra, C. A. van Blitterswijk, M. Karperien and J. Feijen, *Acta Biomater.*, 2010, **6**, 1968.
- 22 J. L. Young and A. J. Engler, *Biomaterials*, 2011, **32**, 1002.
- 23 X. Z. Shu, Y. Liu, Y. Luo, M. C. Roberts and G. D. Prestwich, *Biomacromolecules*, 2002, **3**, 1304.
- 24 G. Liang, H. Ren and J. Rao, *Nat. Chem.*, 2009, **2**, 54.
- 25 S.-Y. Choh, D. Cross and C. Wang, *Biomacromolecules*, 2011, **12**, 1126.
- 26 Y. Ma, J. Thiele, L. Abdelmohsen, J. Xu and W. T. S. Huck, *Chem. Commun.*, 2014, **4**, 112.
- 27 J. K. Armstrong, R. B. Wenby, H. J. Meiselman and T. C. Fisher, *Biophys. J.*, 2004, **87**, 4259.
- 28 R. Gabler, E. W. Westhead and N. C. Ford, *Biophys. J.*, 1974, **14**, 528.
- 29 S. C. Blanchard, H. D. Kim, R. L. Gonzalez, Jr., J. D. Puglisi and S. Chu, *Proc. Natl. Acad. Sci. U. S. A.*, 2004, **101**, 12893.
- 30 T. Stögbauer, L. Windhager, R. Zimmer and J. O. Rädler, *Integr. Biol.*, 2012, **4**, 494.
- 31 F. Courtois, L. F. Olguin, G. Whyte, D. Bratton, W. T. S. Huck, C. Abell and F. Hollfelder, *ChemBioChem*, 2008, **9**, 439.
- 32 J. W. Szostak, D. P. Bartel and P. L. Luisi, *Nature*, 2001, **409**, 387.
- 33 V. Noireaux, R. Bar-Ziv, J. Godefroy, H. Salman and A. Libchaber, *Phys. Biol.*, 2005, **2**, P1.
- 34 D. B. Wolfe, D. Qin and G. M. Whitesides, *Methods Mol. Biol.*, 2010, **583**, 81.
- 35 X. Z. Shu, Y. Liu, Y. Luo, M. C. Roberts and G. D. Prestwich, *Biomacromolecules*, 2002, **3**, 1304.
- 36 J. L. Young and A. J. Engler, *Biomaterials*, 2011, **32**, 1002.
- 37 G. L. Ellman, *Arch. Biochem. Biophys.*, 1959, **82**, 70.
- 38 V. Chokkalingam, J. Tel, F. Wimmers, X. Liu, S. Semenov, J. Thiele, C. G. Figdor and W. T. S. Huck, *Lab Chip*, 2013, **13**, 4740.